HARDWARE-IN-THE-LOOP SIMULATION FOR DRIVE WHEEL SLIP CONTROL OF HIGH-POWER TRACTOR FOR PLOUGHING OPERATION

/

基于硬件在环仿真的大马力拖拉机犁耕作业驱动轮滑转控制研究

Shuo ZHANG[1)], YanQing LUO[1)], Lei JIA[1)], JingMing WEN[1)], HongLing JIN[1)], Yu CHEN*[1)]
College of Mechanical and Electronic Engineering, Northwest A&F University, Yangling 712100, China
Tel: +86 17795759790; E-mail: jdxy73@nwafu.edu.cn
DOI: https://doi.org/10.35633/inmateh-75-33

Keywords: *high-power tractor, ploughing operation, slip control, SMVSC, HILS*

ABSTRACT

To address the issue of increased fuel consumption and reduced efficiency caused by excessive slip of the drive wheels during tractor ploughing operations, this paper considered the time-varying, uncertain, and highly nonlinear characteristics of the tractor-operating unit. A nonlinear dynamic model was constructed and a nonlinear slip control method for the drive wheels was designed using sliding mode variable structure control (SMVSC). The method was validated and tested on both the MATLAB/Simulink platform and a hardware-in-the-loop (HIL) simulation platform based on dSPACE. The HILS results indicated that, compared to the fuzzy PID algorithm, under varying soil specific resistance pulses, the mean absolute deviation of slip rate was reduced by 0.013, and the response time decreased by approximately 1.3 seconds with the SMVSC method. In case of pulse variation in slip rate, the SMVSC method reduced the tracking response time by approximately 0.8 seconds and the average control overshoot by about 0.03. Under both experimental conditions, the SMVSC method demonstrated superior control performance, ensuring more stable tractor operation. These findings provide valuable insights for drive slip control in tractor ploughing operations.

摘要

为解决拖拉机犁耕作业时驱动轮过度滑转引起燃油消耗量增加和效率降低的问题，本文考虑拖拉机作业机组时变、不确定和强非线性特征，构建了非线性动力学模型并结合滑模变结构控制设计了驱动轮滑转非线性控制方法，分别在 MATLAB/Simulink 平台以及基于 dSPACE 搭建的硬件在环仿真平台进行验证测试。硬件在环测试结果表明，相比模糊 PID 算法，在土壤比阻脉冲变化时，SMVSC 方法下滑转率的平均绝对值偏差减少了 0.013，响应时间减少了约 1.3s；在滑转率脉冲变化时，SMVSC 方法的跟踪响应时间减少了约 0.8s，平均控制过冲减少了约 0.03。两种试验条件下，SMVSC 的控制效果更佳且能够使拖拉机保持较稳定的作业状态，对于拖拉机犁耕作业中的驱动防滑控制具有一定的参考意义。

INTRODUCTION

With the intelligent and intensive development of modern agriculture *(Giller et al., 2015)*, the heavy tractors have become important tools for efficient operation in field planting *(Janulevičius et al., 2019)*. However, excessive slip of the drive wheels during ploughing operations can significantly reduce the field operation efficiency of heavy tractor unit and negatively affect soil quality *(Rahmati et al., 2020)*. With the deepening of the concept of “Green Agriculture” and the continuous improvement of soil protection requirements *(Wang et al., 2020; Holthusen et al., 2018)*, the introduction and enhancement of intelligent slip control for tractor drive wheels will substantially improve tillage efficiency and optimize soil conditions.

At present, the research on the slip rate is mainly focusing on the measurement and identification method, mathematical modelling, control algorithm, etc. For example, there are relative researches on real-time monitoring of slip rate but not involving automatic control *(Pranav et al., 2010)*, and the traction resistance is adjusted by changing the plough depth at the level of force to meet the purpose of controlling slip rate within a certain range, that it is mainly used by PID, fuzzy control and other methods *(Zhang et al., 2016)*. In the process of mathematical modelling, most of the existing researches employ linearization methods to approximate the nonlinear characteristics of tractor, electro-hydraulic hitch system or operating unit.

[1] *Shuo Zhang, Associate professor, Ph.D. Eng.; YanQing Luo, M.S. Stud. Eng.; Lei Jia, M.S. Stud. Eng.; JingMing Wen, M.S. Stud. Eng.; HongLing Jin, Associate professor, Ph.D. Eng.; Yu Chen, Associate professor, Ph.D. Eng.*

Although there have been some further researches on more accurate drive anti-slip control, the strong nonlinear characteristics of the large complex inertial system are not completely considered *(Watanabe M. and Sakai K., 2019)*, resulting in limited accuracy. Sliding mode variable structure control (SMVSC) is a control method which can solve the nonlinear problem. It is mainly used in the field of agricultural machinery automatic control, such as tractor automatic steering *(He et al., 2023)*, path tracking control *(Ji et al., 2023)* and trajectory tracking considering slip *(Zhang et al., 2022; Ding et al., 2022)*.

In the research on heavy tractor control, the experimental method is also an important part. Due to the difficulty in verifying the real-time execution capability of controllers through offline simulations, field experiments are often relied upon. However, these experiments are influenced by factors such as seasonality and crop growth cycles. Hardware-in-the-loop simulation (HILS), which runs simulation models on real-time processors, can simulate dynamic changes under various experimental conditions and evaluate the performance of control systems and controllers *(Li et al., 2007; Paksoy et al., 2020)*. Now it is gradually trying to provide test solutions for special equipment in the agricultural field. *Raikwar et al., (2019),* developed a set of HILS test platform based on the automatic test of tractor embedded system to detect and evaluate the faults or defects of tractor electronic control units and control functions. *Wu et al., (2019),* developed a hardware-in-loop test platform using digital space as a tool to test and verify the efficiency of the power system management unit of electric tractor. *Xu et al., (2021),* proposed a layered multi-loop robust control architecture (LMLRC) for tractor path following control, and built a hardware-in-the-loop simulation platform with MicroAutoBox, PXI hardware, LabVIEW and other tools, based on which the dynamic effectiveness of the proposed controller was verified. *Zhang et al., (2023),* tested the proposed active torque distribution control strategy on the dSPACE hardware-in-the-loop simulation platform, demonstrating the controller's obvious advantages in reducing tractor slip, improving traction energy efficiency, and reducing motor energy consumption.

Based on the research of the "tractor-tool-soil" system, this paper has developed a dynamic model of a high-power tractor with electro-hydraulic hitch system during ploughing operations. A slip rate control strategy has been proposed based on this model and the SMVSC theory. Finally, offline simulations and hardware-in-the-loop tests have been conducted on the MATLAB/Simulink and dSPACE platforms, respectively, using a fuzzy PID control method for comparison. The experimental results of both methods have been compared, leading to the optimization of the anti-slip control for the drive wheels of high-power tractors.

MATERIALS AND METHODS

Description of the HILS

The HILS test platform is composed of two parts: software and hardware. The software part encompasses the mathematical model of a half-vehicle, the control algorithm, and the MATLAB-Simulink software. On the hardware side, the platform is equipped with a dSPACE DS1007 serving as the main processor, along with a power supply, an AD conversion board DS2002, a DA conversion board DS2103, a CAN module DS4302, and a controller based on the Freescale MC9S12XS128MAL. The schematic diagram of the entire system is presented in Figure 1.

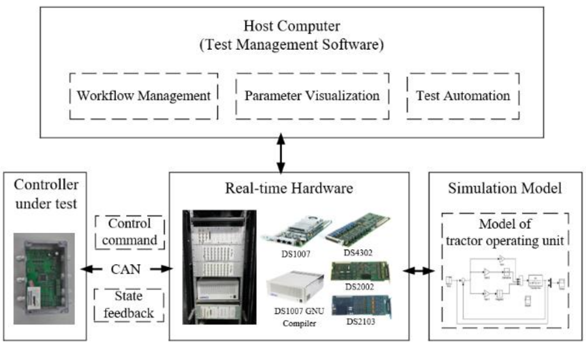

Fig. 1 - Schematic diagram of HILS

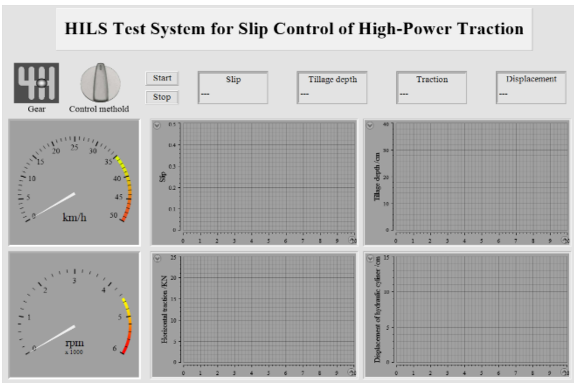

Fig. 2 - The human-machine interface of HILS

The specific functions of the system are as follows: the Tractor simulation model runs in the dSPACE real-time operating environment to simulate the dynamic response characteristics of the tractor under different working conditions; the test management software based on ControlDesk runs in the PC environment of the host computer to provide a good human-computer interaction interface, which can monitor system running state and controller performance in real time, display and dynamically modify system model parameters, and realize workflow management and test automation. The dSPACE real-time processor interfaces with the controller through I/O interface (CAN bus) to realize the signal communication between the real-time model of tractor and the actual controller. In addition, the human-machine interface (as shown in figure 2) is designed based on the ControlDesk, including the functions of adjusting control parameters, displaying the status of the control system (tractor slip rate, tillage depth, etc.), tracking process response curve, etc.

The half-tractor model

In the mathematical modelling of heavy tractor electro-hydraulic hitch operation units, it is considered that the tractor works in the field mostly in a straight-line motion, and the field road environment is relatively flat. Therefore, the tractor’s motion is simplified to linear motion in the longitudinal plane along the tractor's forward direction, ignoring the lateral movements such as sideslip and roll during forward movement. As shown in figure 3, the centre point of the rear axle is used as the coordinate origin to establish the x_O-O-y_O motion coordinate of the tractor's electro-hydraulic hitch operation units.

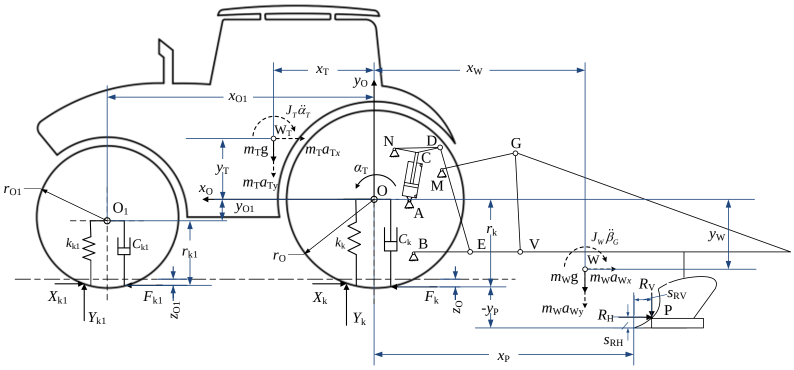

Fig. 3 - Simple diagram of kinematic and dynamic analysis for heavy tractor

- **Kinematics analysis**

The motion of the heavy tractor electro-hydraulic hitch operation unit is simplified into two parts: one is the tractor's translational motion in the forward direction with the base point *O*, the other is the rotational motion of the tractor's linkage around the base point *O* in the longitudinal plane, and the relative position relationship of the tractor's main points is expressed by the tractor's relative position relationship when driving on the flat ground. According to the basic theory of kinematics, for each main node of tractor and its linkage, its velocity can be expressed as the velocity projection component of the point and the base point *O* in the line direction, and its acceleration can be expressed as the vector sum of the acceleration of the base point *O* and the rotational acceleration of the point around the point *O*.

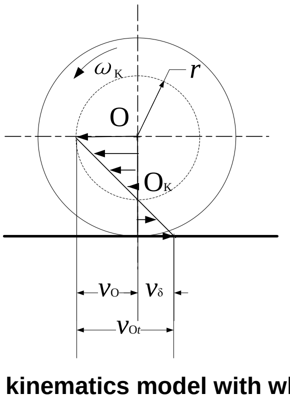

Fig. 4 - Rolling kinematics model with wheels slipping

When the tractor is ploughing, it has the characteristics of approximately constant speed linear operation, so its motion state is generally a rolling motion state with slip, as shown in figure 4. Assuming that during the movement, the instantaneous centre point of the speed of the tractor drive wheel is always above the soil ground in the field, the wheel slip rate of the rear-wheel drive tractor can be expressed as by equation (1):

$$\delta_K = \frac{v_{Ot} - v_O}{v_{Ot}} = \frac{r_O \omega_K - r_K \omega_K}{r_O \omega_K} = 1 - \frac{r_K}{r_O} \tag{1}$$

where: V_{Ot} and V_O are respectively the theoretical speed and instantaneous speed of the drive wheel in the forward direction, m/s; r_O and r_K are respectively the geometric radius and dynamic radius of the drive wheel, m; ω_K is the angular speed of the drive wheel, rad/s.

As shown in Fig. 5, based on the analysis of the geometric relationship model between the piston displacement of the lifting hydraulic cylinder and the position of hitch pole with changes of the farm tools' depth, the relationship between above three can be approximately obtained. On the basis of abovementioned geometric relation, the displacement of lifting hydraulic cylinder is $x_L=x_{L0}$ when the farming tool is in the predetermined tillage depth. The first-order and second-order differential relation of the angle and movement displacement of each member can be derived. Due to space limitations, the differential equations are no longer listed here.

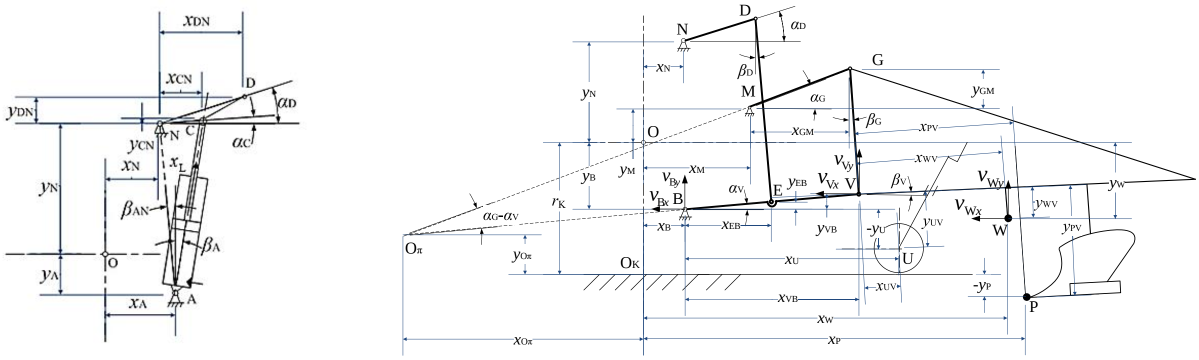

(a) *Lifting hydraulic cylinder and lifting arm* (b) *The lifting and drag rob, farm tools*

Fig. 5 - Simple diagram of kinematic and dynamic analysis for heavy tractor

NCD is the lifting arm; DE is the lifting rod; MG is the drag rob; BV is the horizontal bar; G and V are the hitch points connecting the upper and lower pull rods and farm tools; W is centroid of farm tools; x_L is the displacement of hydraulic cylinder piston; x_W, y_W are the horizontal and vertical distances from the rear wheel axis O to the centroid, m; α_C, α_D, α_V, α_G, β_V are the angles between the corresponding member and the horizontal direction, rad; β_A, β_D, β_G are the angles between the corresponding member and the horizontal direction, rad.

- **Dynamic analysis**

In Figure 3, the force analysis of the tractor's electro-hydraulic hitch operation unit shows that the external forces received by the tractor (including the hitch mechanism) mainly include: the tractor's gravity m_{Tg}, the farm tools' gravity m_{Wg}, the front wheels' vertical ground reaction Y_{K1}, the horizontal rolling resistance X_{K1} and the corresponding driving force F_{k1}, the rear wheels' vertical ground reaction Y_K, the horizontal rolling resistance X_K and the corresponding driving force F_K, and the farm tools' soil resistance R_H and R_V, the force F_G, F_{vx} and F_{vy} of the tool on the linkage at the upper and lower hitch points. Therefore, with the point *O* as the centre, the force and moment balance equations in the horizontal and vertical directions have been set up, as shown in equation (2).

$$\begin{cases} Y_K + Y_{K1} - R_V = m_T\left(g + a_{Ty}\right) + m_W\left(g + a_{Wy}\right) \\ F_K + F_{K1} - X_K - X_{K1} - R_H = m_T a_{Tx} + m_W a_{Wx} \\ R_H\left(r_K - y_P - s_{R_H}\right) - R_V\left(x_P + s_{R_V}\right) - \left(F_K + F_{K1}\right)r_K + X_{K1}y_{O1} - Y_{K1}x_{O1} \\ +m_T\left(g + a_{Ty}\right)x_T - m_T a_{Tx} y_T - m_W\left(g + a_{Wy}\right)x_W + m_W a_{Wx} y_W = J_T\ddot{\alpha}_T + J_W\ddot{\beta}_G \end{cases} \tag{2}$$

According to the above relevant kinematics and dynamics analysis, and referring to the previous research results and modelling methods, the kinematics and dynamics equations of each subsystem such as the tractor body, wheels, hitch mechanism and agricultural tools are brought into equation (2). The dynamic differential equations of tractor electro-hydraulic hitch ploughing unit are obtained, as shown in formula (3). In this formula, Y_K and $Y_{\Delta K}$ are intermediate variables; s_{O1} and s_o are respectively the compression deformation of front and rear tires, m; z_{o1} and z_o are respectively the soil subsidence caused by vertical load of front and rear tires, m; A_{K1} and A_K are the grounding area of front and rear tires, m^2; B_{K1} and B_K are respectively the grounding width of front and rear tires, m. The coefficients such as m_{x_Le}, $i_{x_LY_K}$, $J'_{x_L\alpha_Le}$, $l_{\alpha_T F_K}$ are respectively the intermediate equivalent mass, equivalent moment of inertia and other equivalent coefficients appearing in the process of solving the equation system, which can be expressed as expressions of known variables or constants. This study based on the author's previous work, utilizing the key dimensions and structural parameters of the tractor operating unit as outlined in reference *(Zhang et al., 2020)*. Due to space constraints, further details are omitted.

$$
\begin{cases}
\ddot{x}_{\mathrm{L}} = \dfrac{1}{m_{x_{\mathrm{L}}e}}\left[p_{\mathrm{L}}A_{\mathrm{L}} + i_{x_{\mathrm{L}}F_{\mathrm{K}}}\left(F_{\mathrm{K}}+F_{\mathrm{K1}}\right) + i_{x_{\mathrm{L}}R_{\mathrm{H}}}R_{H} - i_{x_{\mathrm{L}}Y_{\mathrm{K}}}Y_{\mathrm{K}} - i_{x_{\mathrm{L}}Y_{\mathrm{K1}}}Y_{\mathrm{K1}} - i_{x_{\mathrm{L}}R_{\mathrm{V}}}R_{V} - m_{x_{\mathrm{L}}g}g - J'_{x_{\mathrm{L}}\alpha_{\mathrm{L}}e}a_T^{\,2} - m_{x_{\mathrm{L}}\alpha_{\mathrm{L}}e}\dot{x}_{\mathrm{L}}\dot{a}_T - m'_{x_{\mathrm{L}}e}\dot{x}_{\mathrm{L}}^2\right] \\
\dot{\delta}_{\mathrm{K}} = \left(1-\delta_{\mathrm{K}}\right)\left(\dfrac{\dot{\omega}_{\mathrm{K}}}{\omega_{\mathrm{K}}} - \dfrac{\dot{s}_{\mathrm{O}}}{r_{\mathrm{O}}-s_{\mathrm{O}}}\right) + \dfrac{1}{\omega_{\mathrm{K}}\left(r_{\mathrm{O}}-s_{\mathrm{O}}\right)\left(m_{\mathrm{T}}+m_{\mathrm{W}}\right)}\left\{\dfrac{m_{x_{\mathrm{O}}x_{\mathrm{L}}}}{m_{x_{\mathrm{L}}e}}p_{\mathrm{L}}A_{\mathrm{L}} + \left(i_{x_{\mathrm{O}}R_{\mathrm{H}}} + i_{x_{\mathrm{L}}R_{\mathrm{H}}}\dfrac{m_{x_{\mathrm{O}}x_{\mathrm{L}}}}{m_{x_{\mathrm{L}}e}}\right)R_{\mathrm{H}} + \left(i_{x_{\mathrm{O}}Y_{\mathrm{K}}} - i_{x_{\mathrm{L}}Y_{\mathrm{K}}}\dfrac{m_{x_{\mathrm{O}}x_{\mathrm{L}}}}{m_{x_{\mathrm{L}}e}}\right)Y_{\mathrm{K}}\right. \\
\quad + \left(i_{x_{\mathrm{O}}Y_{\mathrm{K1}}} - i_{x_{\mathrm{L}}Y_{\mathrm{K1}}}\dfrac{m_{x_{\mathrm{O}}x_{\mathrm{L}}}}{m_{x_{\mathrm{L}}e}}\right)Y_{\mathrm{K1}} + \left(l_{x_{\mathrm{O}}}^{-1}y_{\mathrm{T}}m_{\mathrm{T}} - m_{x_{\mathrm{L}}g}\dfrac{m_{x_{\mathrm{O}}x_{\mathrm{L}}}}{m_{x_{\mathrm{L}}e}}\right)g - \left(i_{x_{\mathrm{O}}F_{\mathrm{K}}} - i_{x_{\mathrm{L}}F_{\mathrm{K}}}\dfrac{m_{x_{\mathrm{O}}x_{\mathrm{L}}}}{m_{x_{\mathrm{L}}e}}\right)\left(F_{\mathrm{K}}+F_{\mathrm{K1}}\right) - \left(i_{x_{\mathrm{O}}R_{\mathrm{V}}} + i_{x_{\mathrm{L}}R_{\mathrm{V}}}\dfrac{m_{x_{\mathrm{O}}x_{\mathrm{L}}}}{m_{x_{\mathrm{L}}e}}\right)R_{\mathrm{V}} \\
\quad \left. + \left(m'_{x_{\mathrm{O}}x_{\mathrm{L}}} - m'_{x_{\mathrm{L}}e}\dfrac{m_{x_{\mathrm{O}}x_{\mathrm{L}}}}{m_{x_{\mathrm{L}}e}}\right)\dot{x}_{\mathrm{L}}^2 - \left(J_{x_{\mathrm{O}}\alpha_{\mathrm{T}}} + J'_{x_{\mathrm{L}}\alpha_{\mathrm{L}}e}\dfrac{m_{x_{\mathrm{O}}x_{\mathrm{L}}}}{m_{x_{\mathrm{L}}e}}\right)a_T^{\,2} + \left(m_{x_{\mathrm{O}}\alpha_{\mathrm{T}}x_{\mathrm{L}}} - m_{x_{\mathrm{L}}\alpha_{\mathrm{L}}e}\dfrac{m_{x_{\mathrm{O}}x_{\mathrm{L}}}}{m_{x_{\mathrm{L}}e}}\right)\dot{x}_{\mathrm{L}}\dot{a}_T\right\} \\
\ddot{y}_{\mathrm{K}} = \ddot{y}_{\mathrm{O}R} + \dfrac{1}{m_{\mathrm{T}}+m_{\mathrm{W}}}\left\{\dfrac{m_{y_{\mathrm{O}}x_{\mathrm{L}}}}{m_{x_{\mathrm{L}}e}}p_{\mathrm{L}}A_{\mathrm{L}} - \left(i_{y_{\mathrm{O}}R_{\mathrm{H}}} - i_{x_{\mathrm{L}}R_{\mathrm{H}}}\dfrac{m_{y_{\mathrm{O}}x_{\mathrm{L}}}}{m_{x_{\mathrm{L}}e}}\right)R_{\mathrm{H}} - \left(i_{y_{\mathrm{O}}Y_{\mathrm{K}}} + i_{x_{\mathrm{L}}Y_{\mathrm{K}}}\dfrac{m_{y_{\mathrm{O}}x_{\mathrm{L}}}}{m_{x_{\mathrm{L}}e}}\right)Y_{\mathrm{K}} - \left(i_{y_{\mathrm{O}}Y_{\mathrm{K1}}} + i_{x_{\mathrm{L}}Y_{\mathrm{K1}}}\dfrac{m_{y_{\mathrm{O}}x_{\mathrm{L}}}}{m_{x_{\mathrm{L}}e}}\right)Y_{\mathrm{K1}}\right. \\
\quad + \left(i_{y_{\mathrm{O}}F_{\mathrm{K}}} + i_{x_{\mathrm{L}}F_{\mathrm{K}}}\dfrac{m_{y_{\mathrm{O}}x_{\mathrm{L}}}}{m_{x_{\mathrm{L}}e}}\right)\left(F_{\mathrm{K}}+F_{\mathrm{K1}}\right) + \left(i_{y_{\mathrm{O}}R_{\mathrm{V}}} - i_{x_{\mathrm{L}}R_{\mathrm{V}}}\dfrac{m_{y_{\mathrm{O}}x_{\mathrm{L}}}}{m_{x_{\mathrm{L}}e}}\right)R_{\mathrm{V}} + \left(m_{y_{\mathrm{O}}g} - m_{x_{\mathrm{L}}g}\dfrac{m_{y_{\mathrm{O}}x_{\mathrm{L}}}}{m_{x_{\mathrm{L}}e}}\right)g + \left(m'_{y_{\mathrm{O}}x_{\mathrm{L}}} - m'_{x_{\mathrm{L}}e}\dfrac{m_{y_{\mathrm{O}}x_{\mathrm{L}}}}{m_{x_{\mathrm{L}}e}}\right)\dot{x}_{\mathrm{L}}^2 \\
\quad \left. + \left(J_{y_{\mathrm{O}}\alpha_{\mathrm{T}}} - J'_{x_{\mathrm{L}}\alpha_{\mathrm{L}}e}\dfrac{m_{y_{\mathrm{O}}x_{\mathrm{L}}}}{m_{x_{\mathrm{L}}e}}\right)a_T^{\,2} + \left(m_{y_{\mathrm{O}}x_{\mathrm{L}}\alpha_{\mathrm{T}}} - m_{x_{\mathrm{L}}\alpha_{\mathrm{L}}e}\dfrac{m_{y_{\mathrm{O}}x_{\mathrm{L}}}}{m_{x_{\mathrm{L}}e}}\right)\dot{x}_{\mathrm{L}}\dot{a}_T\right\} \\
\ddot{y}_{\Delta\mathrm{K}} = \ddot{y}_{\mathrm{O}R} - \ddot{y}_{\mathrm{O1}R} + \dfrac{x_{\mathrm{O1}}}{J_{\alpha_{\mathrm{T}}}}\left\{\dfrac{m_{\alpha_{\mathrm{T}}}}{m_{x_{\mathrm{L}}e}}p_{\mathrm{L}}A_{\mathrm{L}} - \left(l_{\alpha_{\mathrm{T}}R_{\mathrm{H}}} - i_{x_{\mathrm{L}}R_{\mathrm{H}}}\dfrac{m_{\alpha_{\mathrm{T}}}}{m_{x_{\mathrm{L}}e}}\right)R_{\mathrm{H}} - \left(l_{\alpha_{\mathrm{T}}Y_{\mathrm{K}}} + i_{x_{\mathrm{L}}Y_{\mathrm{K}}}\dfrac{m_{\alpha_{\mathrm{T}}}}{m_{x_{\mathrm{L}}e}}\right)Y_{\mathrm{K}} - \left(l_{\alpha_{\mathrm{T}}Y_{\mathrm{K1}}} + i_{x_{\mathrm{L}}Y_{\mathrm{K1}}}\dfrac{m_{\alpha_{\mathrm{T}}}}{m_{x_{\mathrm{L}}e}}\right)Y_{\mathrm{K1}}\right. \\
\quad + \left(l_{\alpha_{\mathrm{T}}F_{\mathrm{K}}} + i_{x_{\mathrm{L}}F_{\mathrm{K}}}\dfrac{m_{\alpha_{\mathrm{T}}}}{m_{x_{\mathrm{L}}e}}\right)\left(F_{\mathrm{K}}+F_{\mathrm{K1}}\right) + \left(y_{\mathrm{T}}m_{\mathrm{T}} + m_{x_{\mathrm{L}}g}\dfrac{m_{\alpha_{\mathrm{T}}}}{m_{x_{\mathrm{L}}e}}\right)g + \left(l_{\alpha_{\mathrm{T}}R_{\mathrm{V}}} - i_{x_{\mathrm{L}}R_{\mathrm{V}}}\dfrac{m_{\alpha_{\mathrm{T}}}}{m_{x_{\mathrm{L}}e}}\right)R_{\mathrm{V}} + \left(m'_{\alpha_{\mathrm{L}}} - m'_{x_{\mathrm{L}}e}\dfrac{m_{\alpha_{\mathrm{T}}}}{m_{x_{\mathrm{L}}e}}\right)\dot{x}_{\mathrm{L}}^2 \\
\quad \left. + \left(J_{\alpha_{\mathrm{T}}\alpha_{\mathrm{T}}} + J_{\alpha_{\mathrm{T}}}\dfrac{y_{\mathrm{O1}}}{x_{\mathrm{O1}}} - J'_{x_{\mathrm{L}}\alpha_{\mathrm{L}}e}\dfrac{m_{\alpha_{\mathrm{T}}}}{m_{x_{\mathrm{L}}e}}\right)a_T^{\,2} + \left(m_{\alpha_{\mathrm{T}}x_{\mathrm{T}}} - m_{x_{\mathrm{L}}\alpha_{\mathrm{L}}e}\dfrac{m_{\alpha_{\mathrm{T}}}}{m_{x_{\mathrm{L}}e}}\right)\dot{x}_{\mathrm{L}}\dot{a}_T\right\} \\
\dot{s}_{\mathrm{O}} = \dfrac{1}{f_{\mathrm{K}}}\left[A_{\mathrm{K}}\left(k_c/B_{\mathrm{K}} + k_{\varphi}\right)z_{\mathrm{O}}^n - k_{\mathrm{K}}s_{\mathrm{O}}\right] \\
\dot{s}_{\mathrm{O1}} = \dfrac{1}{f_{\mathrm{K1}}}\left[A_{\mathrm{K1}}\left(k_c/B_{\mathrm{K1}} + k_{\varphi}\right)z_{\mathrm{O1}}^n - k_{\mathrm{K1}}s_{\mathrm{O1}}\right] \\
z_{\mathrm{O}} = y_{\mathrm{K}} - s_{\mathrm{O}} \\
z_{\mathrm{O1}} = y_{\mathrm{K}} - y_{\Delta\mathrm{K}} - s_{\mathrm{O1}}
\end{cases}
\tag{3}
$$

Slip Rate Controller Design

Through the analysis of the movement characteristics of the heavy tractor ploughing unit, it can be seen that when the soil conditions change suddenly, the tractor slip rate changes greatly, which will seriously affect the tractor's traction performance. Therefore, in view of the nonlinear characteristics of the heavy tractor electro-hydraulic hitch unit, considering the tractor traction efficiency, according to the slip rate control requirements under different ploughing conditions and considering the uniformity of ploughing depth, a slip rate control method with the optimal slip rate δ_{opt}=0.2 as the control target was designed in this paper. The operation principle of the slip rate control system based on the optimal target is shown in figure 6. In this paper, the sliding mode variable structure control method is used to study, and the fuzzy PID control method is added to compare.

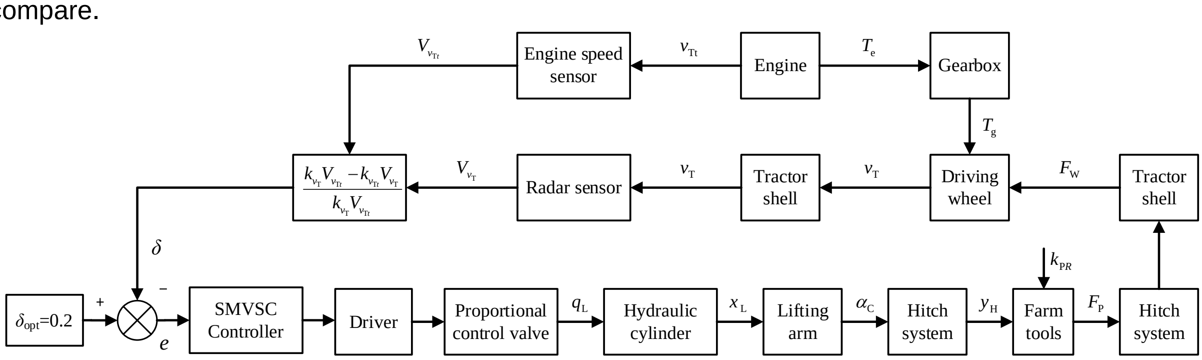

Fig. 6 - Diagram of control system working principle

- **Research on the SMVSC algorithm**

Because there are a lot of physical parameters and uncertainties which are difficult to obtain accurately in the tractor dynamics model, and the system equation has strong nonlinearity, the sliding mode variable structure control method is a nonlinear control method which adapts to the strong nonlinearity and is insensitive to the external disturbance, and has better robustness and higher reliability.

First, the output error is defined as:

$$e=\delta_{\mathrm{K}}-\delta_{\mathrm{opt}} \tag{4}$$

According to the sliding mode variable structure control theory, the switching function is defined as:

$$s(t)=Ce=C(\delta_{\mathrm{K}}-\delta_{\mathrm{opt}}) \tag{5}$$

where:

C is the sliding mode coefficient, and C >0, setting C =1.

The design of the sliding mode variable structure controller consists of two main aspects: on the one hand, it needs to be ensured that any position in the phase plane can reach the switching function s=0 in a finite time, and on the other hand, it needs to be ensured that it can converge to an equilibrium point on the switching function. According to the defined switching function and the basic principle of SMVSC, in the phase plane composed of the slip rate and the derivative of the slip rate, the switching line is a straight line with a slope of - C and passing through (δ_{opt}, 0). The basic idea of SMVSC is to select an appropriate control variable, so that during the operation of the tractor, its phase trajectory (δ_k, $\dot{\delta}$) continuously slides along the switching line to the control target (δ_{opt}, 0) by a predetermined control law. Derivation of equation (5) gives:

$$\dot{s}(t)=C\dot{e}=\dot{\delta}_{\mathrm{K}} \tag{6}$$

Based on the requirement that points in the state space need to be allowed finite time to reach the termination point on the switching function s=0, the following conditions must be satisfied when designing the controller: when $s(t)$>0,

$$\dot{s}(t)=C\dot{e}=\dot{\delta}_{\mathrm{K}}<0 \tag{7}$$

When $s(t)$<0,

$$\dot{s}(t)=C\dot{e}=\dot{\delta}_{\mathrm{K}}>0 \tag{8}$$

Substituting the first-order differential equation expression of the slip rate that has been derived from the dynamic model into equation (6) gives:

$$\begin{aligned}\dot{s}(t)=&\left(1-\delta_{\mathrm{K}}\right)\left(\frac{\dot{\omega}_{\mathrm{K}}}{\omega_{\mathrm{K}}}-\frac{\dot{s}_{\mathrm{O}}}{r_{\mathrm{O}}-s_{\mathrm{O}}}\right)+\frac{1}{\omega_{\mathrm{K}}\left(r_{\mathrm{O}}-s_{\mathrm{O}}\right)\left(m_{\mathrm{T}}+m_{\mathrm{W}}\right)}\left\{\frac{m_{x_{\mathrm{O}}x_{\mathrm{L}}}}{m_{x_{\mathrm{L}}e}}p_{\mathrm{L}}A_{\mathrm{L}}+\left(i_{x_{\mathrm{O}}R_{\mathrm{H}}}+i_{x_{\mathrm{L}}R_{\mathrm{H}}}\frac{m_{x_{\mathrm{O}}x_{\mathrm{L}}}}{m_{x_{\mathrm{L}}e}}\right)R_{\mathrm{H}}\right.\\&-\left(i_{x_{\mathrm{O}}R_{\mathrm{V}}}+i_{x_{\mathrm{L}}R_{\mathrm{V}}}\frac{m_{x_{\mathrm{O}}x_{\mathrm{L}}}}{m_{x_{\mathrm{L}}e}}\right)R_{\mathrm{V}}-\left(i_{x_{\mathrm{O}}F_{\mathrm{K}}}-i_{x_{\mathrm{L}}F_{\mathrm{K}}}\frac{m_{x_{\mathrm{O}}x_{\mathrm{L}}}}{m_{x_{\mathrm{L}}e}}\right)F_{\mathrm{K}}+\left(i_{x_{\mathrm{O}}Y_{\mathrm{K}}}-i_{x_{\mathrm{L}}Y_{\mathrm{K}}}\frac{m_{x_{\mathrm{O}}x_{\mathrm{L}}}}{m_{x_{\mathrm{L}}e}}\right)Y_{\mathrm{K}}+\left(i_{x_{\mathrm{O}}Y_{\mathrm{K1}}}-i_{x_{\mathrm{L}}Y_{\mathrm{K1}}}\frac{m_{x_{\mathrm{O}}x_{\mathrm{L}}}}{m_{x_{\mathrm{L}}e}}\right)Y_{\mathrm{K1}}\\&\left.-m_{x_{\mathrm{L}}g}\frac{m_{x_{\mathrm{O}}x_{\mathrm{L}}}}{m_{x_{\mathrm{L}}e}}g+\left(m'_{x_{\mathrm{O}}x_{\mathrm{L}}}-m'_{x_{\mathrm{L}}e}\frac{m_{x_{\mathrm{O}}x_{\mathrm{L}}}}{m_{x_{\mathrm{L}}e}}\right)\dot{x}_{\mathrm{L}}^{2}+\left(m_{x_{\mathrm{O}}\alpha_{\mathrm{T}}x_{\mathrm{L}}}-m_{x_{\mathrm{L}}\alpha_{\mathrm{T}}e}\frac{m_{x_{\mathrm{O}}x_{\mathrm{L}}}}{m_{x_{\mathrm{L}}e}}\right)\dot{x}_{\mathrm{L}}\dot{\alpha}_{\mathrm{T}}-\left(J_{x_{\mathrm{O}}\alpha_{\mathrm{T}}}+J'_{x_{\mathrm{L}}\alpha_{\mathrm{T}}e}\frac{m_{x_{\mathrm{O}}x_{\mathrm{L}}}}{m_{x_{\mathrm{L}}e}}\right)\dot{\alpha}_{\mathrm{T}}^{2}\right\}\end{aligned} \tag{9}$$

In order to ensure the stability of the sliding mode motion and the working quality, the dynamic effect of the convergence motion is improved by using the exponential approach law, and constant velocity approaches law is introduced to determine the convergence speed to be a certain non-zero speed when $s(\delta)$ continuously approaching 0, which ensures that the control system arrives at the switching manifold as soon as possible with this speed. The exponential approach law used is shown in equation (10).

$$\dot{s}(t)=-\varepsilon\,\mathrm{sgn}(s(t))-ks(t) \tag{10}$$

where:

ε represents the law of constant velocity approach of the moving point, and ε>0; k represents the law of exponential approach, and k>0; sgn($s(t)$) represents the sign function.

Combine the vertical (9) and (10), and select the piston pressure $p_L A_L$ in the oil chamber of the lifting hydraulic cylinder as the equivalent control quantity, and get:

$$p_{\mathrm{L}}A_{\mathrm{L}}=\omega_{\mathrm{K}}\left(r_{\mathrm{O}}-s_{\mathrm{O}}\right)\left(m_{\mathrm{T}}+m_{\mathrm{W}}\right)\frac{m_{x_{\mathrm{L}}e}}{m_{x_{\mathrm{O}}x_{\mathrm{L}}}}\left(-\varepsilon\,\mathrm{sgn}(s(t))-ks(t)\right)-\omega_{\mathrm{K}}\left(r_{\mathrm{O}}-s_{\mathrm{O}}\right)\left(m_{\mathrm{T}}+m_{\mathrm{W}}\right)\frac{m_{x_{\mathrm{L}}e}}{m_{x_{\mathrm{O}}x_{\mathrm{L}}}}\left(1-\delta_{\mathrm{K}}\right)\left(\frac{\dot{\omega}_{\mathrm{K}}}{\omega_{\mathrm{K}}}-\frac{\dot{s}_{\mathrm{O}}}{r_{\mathrm{O}}-s_{\mathrm{O}}}\right)$$
$$-\left(i_{x_{\mathrm{L}}R_{\mathrm{H}}}+i_{x_{\mathrm{O}}R_{\mathrm{H}}}\frac{m_{x_{\mathrm{L}}e}}{m_{x_{\mathrm{O}}x_{\mathrm{L}}}}\right)R_{\mathrm{H}}+\left(i_{x_{\mathrm{L}}R_{\mathrm{V}}}+i_{x_{\mathrm{O}}R_{\mathrm{V}}}\frac{m_{x_{\mathrm{L}}e}}{m_{x_{\mathrm{O}}x_{\mathrm{L}}}}\right)R_{\mathrm{V}}+\left(i_{x_{\mathrm{O}}F_{\mathrm{K}}}\frac{m_{x_{\mathrm{L}}e}}{m_{x_{\mathrm{O}}x_{\mathrm{L}}}}-i_{x_{\mathrm{L}}F_{\mathrm{K}}}\right)F_{\mathrm{K}}+\left(i_{x_{\mathrm{L}}Y_{\mathrm{K}}}-i_{x_{\mathrm{O}}Y_{\mathrm{K}}}\frac{m_{x_{\mathrm{L}}e}}{m_{x_{\mathrm{O}}x_{\mathrm{L}}}}\right)Y_{\mathrm{K}}$$
$$+\left(m'_{x_{\mathrm{O}}x_{\mathrm{L}}}\frac{m_{x_{\mathrm{L}}e}}{m_{x_{\mathrm{O}}x_{\mathrm{L}}}}-m'_{x_{\mathrm{L}}e}\right)\dot{x}_{\mathrm{L}}^{2}-\left(m_{x_{\mathrm{O}}\alpha_{\mathrm{T}}x_{\mathrm{L}}}\frac{m_{x_{\mathrm{L}}e}}{m_{x_{\mathrm{O}}x_{\mathrm{L}}}}-m_{x_{\mathrm{L}}\alpha_{\mathrm{T}}e}\right)\dot{x}_{\mathrm{L}}\dot{\alpha}_{\mathrm{T}}+\left(J_{x_{\mathrm{O}}\alpha_{\mathrm{T}}}\frac{m_{x_{\mathrm{L}}e}}{m_{x_{\mathrm{O}}x_{\mathrm{L}}}}+J'_{x_{\mathrm{L}}\alpha_{\mathrm{T}}e}\right)\dot{\alpha}_{\mathrm{T}}^{2} \tag{11}$$

It can be seen from equation (11) that the expression is extremely complex. According to the dynamic characteristics of the motion of the electro-hydraulic hitch system and the characteristics of the sliding mode variable structure control theory, it is assumed that the tractor ploughing operation in the field is approximately constant speed operation, that is, the slip rate is kept near the optimal value with small fluctuation. Assume that the tractor engine speed is constant. Assuming that the tractor's pitching motion in the forward longitudinal plane is small, it is considered that the hydraulic cylinder push rod extends at a nearly uniform speed. Through simulation analysis and calculation, it can be further simplified:

$$p_{\mathrm{L}}A_{\mathrm{L}}=k_{1}*\left(-\varepsilon\,\mathrm{sgn}(s(t))-ks(t)\right)+k_{2}v_{\mathrm{O}}+k_{3}R_{\mathrm{H}}+k_{4}R_{\mathrm{V}}+k_{5}F_{\mathrm{K}}+k_{6}Y_{\mathrm{K}}+k_{7}Y_{\mathrm{K1}} \tag{12}$$

where: k_1, k_2, k_3, k_4, k_5, k_6 and k_7 are the coefficients related to tractor structural parameters, which are specifically expressed as follows:

$$k_{1}=\omega_{\mathrm{K}}r_{\mathrm{K}}\left(m_{\mathrm{T}}+m_{\mathrm{W}}\right)\frac{m_{x_{\mathrm{L}}e}}{m_{x_{\mathrm{O}}x_{\mathrm{L}}}},\quad k_{2}=r_{\mathrm{K}}\dot{s}_{\mathrm{O}}\frac{m_{x_{\mathrm{L}}e}}{m_{x_{\mathrm{O}}x_{\mathrm{L}}}}\left(m_{\mathrm{T}}+m_{\mathrm{W}}\right),\quad k_{3}=-i_{x_{\mathrm{L}}R_{\mathrm{H}}}-i_{x_{\mathrm{O}}R_{\mathrm{H}}}\frac{m_{x_{\mathrm{L}}e}}{m_{x_{\mathrm{O}}x_{\mathrm{L}}}},$$
$$k_{4}=i_{x_{\mathrm{L}}R_{\mathrm{V}}}+i_{x_{\mathrm{O}}R_{\mathrm{V}}}\frac{m_{x_{\mathrm{L}}e}}{m_{x_{\mathrm{O}}x_{\mathrm{L}}}},\ k_{5}=i_{x_{\mathrm{O}}F_{\mathrm{K}}}\frac{m_{x_{\mathrm{L}}e}}{m_{x_{\mathrm{O}}x_{\mathrm{L}}}}-i_{x_{\mathrm{L}}F_{\mathrm{K}}},\ k_{6}=i_{x_{\mathrm{L}}Y_{\mathrm{K}}}-i_{x_{\mathrm{O}}Y_{\mathrm{K}}}\frac{m_{x_{\mathrm{L}}e}}{m_{x_{\mathrm{O}}x_{\mathrm{L}}}},\ k_{7}=i_{x_{\mathrm{L}}Y_{\mathrm{K1}}}-i_{x_{\mathrm{O}}Y_{\mathrm{K1}}}\frac{m_{x_{\mathrm{L}}e}}{m_{x_{\mathrm{O}}x_{\mathrm{L}}}}.$$

The Lyapunov function is constructed based on the positive definite function to test the stability of the system employing the exponential convergence rate, and the Lyapunov function is:

$$V=\frac{1}{2}s^{2} \tag{13}$$

Derivatives can be obtained:

$$\dot{V}=\frac{1}{2}\frac{\mathrm{d}}{\mathrm{d}t}s^{2}=s\dot{s}<-\varepsilon\,|\,s\,|<0 \tag{14}$$

where: ε>0.

According to Lyapunov stability theory, it can be concluded that the designed control system is stable.

When the system enters the sliding mode motion and continuously switches along the sliding mode surface, in order to suppress the system "shaking" as much as possible, the continuous saturation function $sat(s)$ is used instead of the traditional constant velocity approach rate discontinuous symbol function $sgn(s)$, which is defined as follows:

$$sat\left(s\right)=\begin{cases}1, & s>\psi\\ s/\psi, & |\,s\,|\leq\psi\\ -1, & s<-\psi\end{cases} \tag{15}$$

where: ψ is the thickness of the boundary layer.

The expression of the equivalent control variable p_LA_L has been derived. The self-developed threaded plug-in proportional control valve was used for indoor testing. Based on the dynamic and static characteristics of the proportional control valve, the opening pressure of the proportional relief valve connected to the oil outlet of the proportional control valve was adjusted. The pressure difference between the load pressure of the proportional lowering control valve and the return oil pressure was controlled to maintain approximately 4 MPa and 9 MPa, respectively. By varying the input voltage of the proportional amplifier (driver), the steady flow of the proportional lowering valve under different driving voltages was obtained. Similarly, the steady flow of the proportional poppet under different driving voltages was measured. Through regression analysis and fitting of the test results, the relationship between control voltage and output flow was determined as follows:

$$U_{\mathrm{up}}=\begin{cases}\dfrac{Q_{up}}{0.475\sqrt{\dfrac{2}{\rho}\Delta p}}+3.87, & 0\le\dfrac{Q_{up}}{\sqrt{\dfrac{2}{\rho}\Delta p}}\le 0.312\\ \dfrac{Q_{up}}{0.475\sqrt{\dfrac{2}{\rho}\Delta p}}+4.27, & \dfrac{Q_{up}}{\sqrt{\dfrac{2}{\rho}\Delta p}}>0.312\end{cases} \tag{16}$$

$$U_{\mathrm{down}}=\begin{cases}1.73-\dfrac{Q_{\mathrm{down}}}{0.48\sqrt{\dfrac{2}{\rho}\left(p_{\mathrm{L}}-p_0\right)}}, & 0\le\dfrac{Q_{\mathrm{down}}}{\sqrt{\dfrac{2}{\rho}\left(p_{\mathrm{L}}-p_0\right)}}\le 0.304\\ 1.27-\dfrac{Q_{\mathrm{down}}}{0.48\sqrt{\dfrac{2}{\rho}\left(p_{\mathrm{L}}-p_0\right)}}, & \dfrac{Q_{\mathrm{down}}}{\sqrt{\dfrac{2}{\rho}\left(p_{\mathrm{L}}-p_0\right)}}>0.304\end{cases} \tag{17}$$

where: U_{up} is the driving voltage of proportional poppet, V; U_{down} is the driving voltage of the proportional lowering valve, V; Q_{up} is the flow of hydraulic oil from the proportional lift valve into the hydraulic cylinder during the lifting process of the hydraulic cylinder, m^3/s; Q_{down} is the flow from the hydraulic cylinder into the proportional descent control valve during the descent of the hydraulic cylinder, m^3/s; $\triangle p$ is the pressure difference between the two ends of the proportional directional valve, and the value has been set 1.5MPa; p_L is the load pressure of the hydraulic cylinder, Pa; p_0 is the return oil pressure, value 0 Pa; ρ is the density of hydraulic oil, kg/m^3.

The flow continuity equation of hydraulic cylinder is shown in equation (18):

$$\dot{p}_{\mathrm{L}}=\frac{\beta_e}{V_{\mathrm{L}}}\left(q_{\mathrm{L}}-A_{\mathrm{L}}\dot{x}_{\mathrm{L}}-C_{\mathrm{tL}}p_{\mathrm{L}}\right) \tag{18}$$

q_L can be obtained by combining equation (12) and equation (18). When the poppet valve is open, q_L=q_{up} (U); when the drop valve is open, q_L=-q_{down}(U). From the equations (16) and (17), the control voltage U of the electro-hydraulic proportional control valve can be obtained to implement the control.

- **Incremental fuzzy PID control method**

In order to highlight the advantages of SMVSC, PID control algorithm which is widely used in control field is selected for comparison. The fuzzy PID controller can improve the robustness of the system in the control process, taking the deviation e and the deviation change rate e_c of the slip rate as the input, and the three parameter correction quantities ΔK_P, ΔK_I and ΔK_D of the PID as the output. The domains of e and e_c are taken as [-0.6, 0.6], and the output variables ΔK_P, ΔK_I, ΔK_D are set according to experience as [-5, 5]. The tuning principles of PID controller parameters are:

(1) When e is larger and e_c is larger, in order to reduce the system response time and avoid system integral saturation, increase K_P and decrease K_I;

(2) When e decreases gradually, in order to shorten the dynamic adjustment time, reduce overshoot and steady-state oscillation, K_P is reduced and K_I is increased;

(3) When the system begins to approach the target and enters steady-state, in order to obtain a good steady state, improve the ability to resist disturbance, increase K_D.

The fuzzy subsets of e, e_c, ΔK_I and ΔK_D are taken as {NB, NM, NS, ZO, PS, PM, PB}, representing {negative big, negative middle, negative small, zero, positive small, positive middle, positive big}, and the membership functions of all subsets are Gauss membership functions. Use MATLAB's fuzzy inference toolbox to build a fuzzy inference system and edit the membership of input and output variables.

RESULTS AND ANALYSIS

Offline simulation and analysis of control algorithm

According to the established system dynamics model and the designed control algorithm, the corresponding simulation model of slip rate control system is established in MATLAB/Simulink, and the entire system is analysed by off-line simulation. During the simulation process, the disturbance rejection characteristics of the sliding rate control system, that is the change of soil specific resistance input, and the dynamic response characteristics of the control target when the input setting value changes, are mainly concerned. After several adjustments, the parameters of SMVSC are determined as ε=1.2, k=0.01, ψ=0.01, and the initial parameters of fuzzy PID controller are K_P=12, K_I=0.5, K_D=1.5. The initial conditions of the simulation are set as follows: the tractor gear is B2 gear, the initial displacement of the hydraulic cylinder piston rod is 8.83 cm, the initial ploughing depth of the tractor operation is 20 cm, and the simulation time is 50 seconds.

- **Soil specific resistance with pulse change**

The simulation takes δ_{opt}=0.2 as the control target, takes the change of soil specific resistance as the external disturbance input, and sets the steady-state value of the soil specific resistance to 30000 N/m^2. At the beginning of the simulation, the soil specific resistance is added as a pulse signal with an amplitude of 8000 N/m^2, a period of 10s and a duty cycle of 50%. When the soil specific resistance changes, the simulation results are shown in Figure 7.

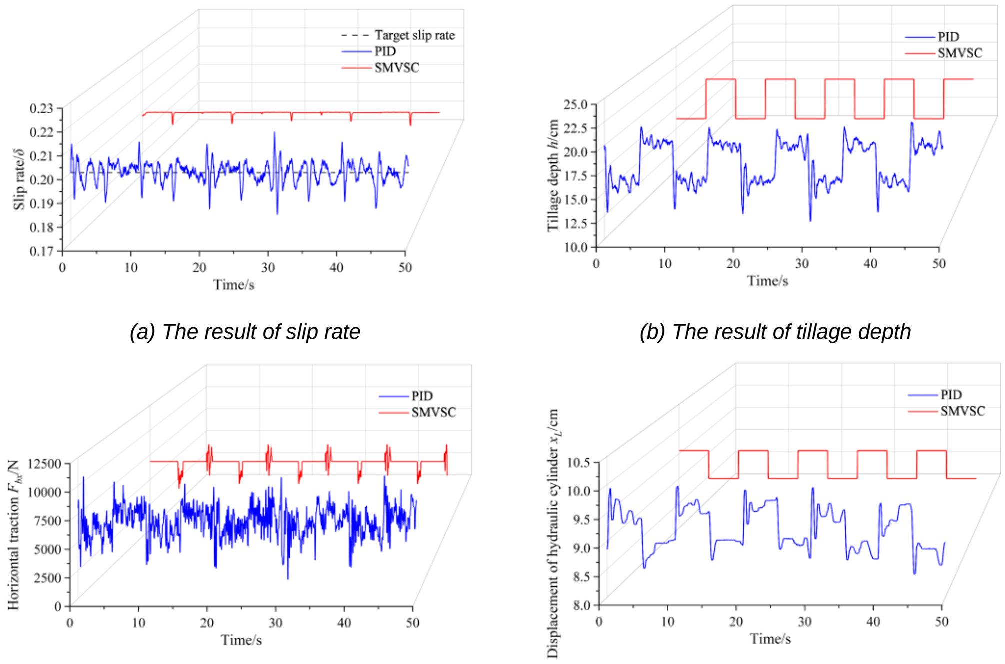

(a) The result of slip rate *(b) The result of tillage depth*

(c) The result of horizontal traction *(d) The result of hydraulic cylinder displacement*

Fig. 7 - Simulation results of soil specific resistance with pulse change

According to Fig. 7 (a), when the specific resistance of soil changes step by step every 5 seconds, through the fuzzy PID control method, after a response time of about 1.5s, the slip rate can be basically controlled around 0.2, but the fluctuation is large, and the maximum error reaches 0.02. The results by the SMVSC method show that the sliding rate can be well controlled at 0.2, and the response time is very short, there is almost no overshoot at the beginning of the control. And the same time, the control target can be continuously and stably tracked in the control process, which can better resist the influence of soil specific resistance disturbance. In addition, when the specific resistance of soil is within 30000N cycle, the dynamic performance of tractor will be affected by random road excitation disturbance, so the fuzzy PID control algorithm can be adjusted according to the magnitude of deviation at any time. The slip rate has been near the target value of 0.2 by large steady-state error. But the SMVSC method has been proven to have a low steady-state error and better robustness against external disturbance, maintaining stability at 0.2 with almost no overshoot. The simulation results showed that when the soil conditions were changing, compared with the fuzzy PID control method, the SMVSC method had better disturbance rejection characteristics and faster response to the external disturbance, which verified the effectiveness and superiority of its control.

- **Control target value with pulse change**

In order to further understand the tracking performance of the control algorithm for the control target, the control target value input by the control system is varied under fixed soil conditions, and the dynamic response characteristics of the control system are analysed when the input undergoes a pulse change. The soil specific resistance is set to 30000 N/m², the initial value of the slip rate control target is 0.2, the control target change amplitude is 0.1, the period is 10s, and the pulse signal has a 50% duty cycle. The simulation results are shown in Figure 8.

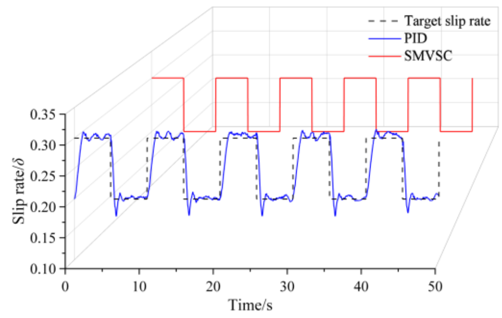

(a) The result of slip rate

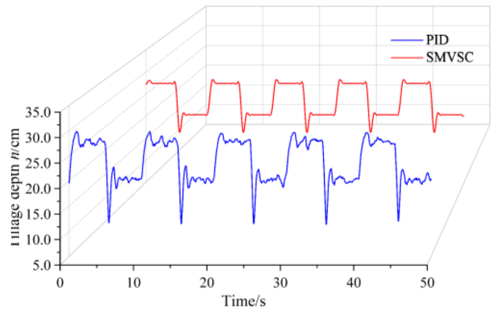

(b) The result of tillage depth

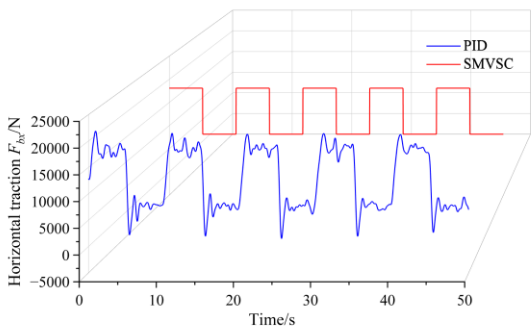

(c) The result of horizontal traction

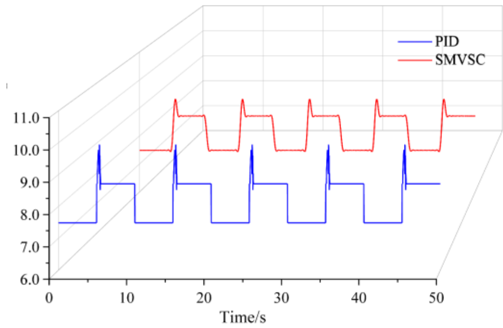

(d) The result of hydraulic cylinder displacement

Fig. 8 - Simulation results of control target value with pulse change

In the control process, the response time of fuzzy PID control was about 1.8s, and the maximum overshoot was 0.05, with a steady-state control error of about 0.01; there was almost no overshoot and steady-state control error by the SMVSC method. When the control target changed periodically between 0.2 and 0.3, the results showed that it reached the control target more quickly by the SMVSC method, the tracking performance of the control target is faster, and the error is smaller. It can be seen that, under certain conditions of the soil without external disturbance, when the control target changes, the dynamic tracking performance to the control target of the SMVSC is better, the response time is shorter than the fuzzy PID control, and there is almost no steady-state error, further proving the SMVSC method superiority.

HILS test and analysis of control algorithm

The HILS test system is used to experimentally investigate the slip rate control for a half-tractor model. According to the test conditions of off-line simulation, based on the HILS real-time simulation test platform, two different algorithms by SMVSC and fuzzy PID control are respectively carried out in the hardware-in-the-loop simulation test, corresponding to the analysis of the sliding rate control when the soil specific resistance pulse changes and the sliding rate control when the control target pulse changes.

- **Soil specific resistance with pulse change**

Setting the same test conditions as the offline simulation, the test duration is 30s, and the results are shown in figure 9.

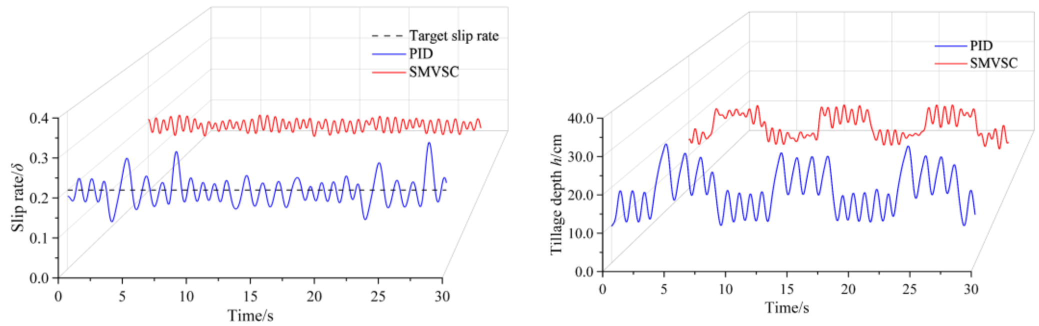

(a) The result of slip rate *(b) The result of tillage depth*

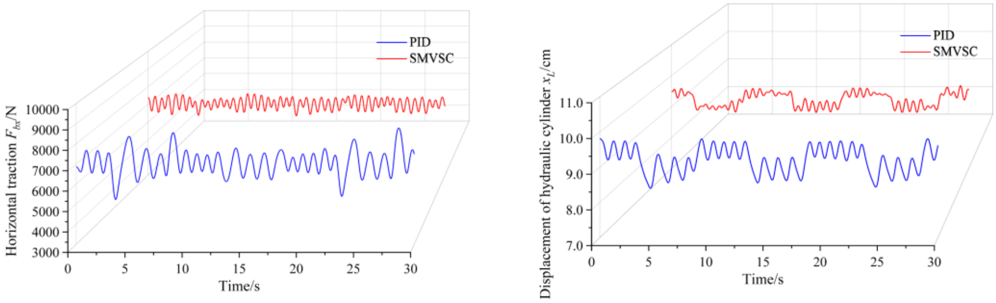

(c) The result of horizontal traction *(d) The result of hydraulic cylinder displacement*

Fig. 9 - HILS results of soil specific resistance with pulse change

The absolute value deviation and variance of the mean value are used as the measurement indicators to evaluate the control effect of the slip rate, and to compare control accuracy of the two different control methods. At the same time, in order to better reflect the status of the ploughing operation under the control of slip rate, the data statistics of ploughing depth, hydraulic cylinder displacement and horizontal traction force were analysed. The analysis results are shown in table 1.

Table 1

Analysis about HILS results

Methods	Slip rate		Tillage depth [cm]		Displacement [cm]		Horizontal traction [N]	
	Mean Absolute Deviation	Variance	Max	Min	Max	Min	Max	Min
SMVS	0.014	0.0002	25.22	11.92	9.67	8.81	7067.78	6350.24
PID	0.027	0.0011	31.46	9.70	9.81	8.40	8783.37	5224.83

By the SMVSC method, the maximum deviation of the slip rate control is 0.041, the mean absolute deviation is 0.014, and the slip rate variance is 0.0002. And by the fuzzy PID control method, the maximum deviation of the slip rate control is 0.121, the average absolute deviation is 0.027, and the slip rate variance is 0.0011. Although the slip rate was controlled around 0.2 through both algorithms, the deviation of the slip rate average absolute value under the SMVSC algorithm is reduced by 48%, the response time is reduced by about 1.3s, and the control deviation is smaller, and the fluctuation amplitude is far smaller than the fuzzy PID control algorithm. In addition, by the SMVSC, the adjustment change of plough depth is 5.26 cm, which is far less than 7.21 cm of fuzzy PID control, reducing about 27%; the adjustment change of hydraulic cylinder displacement is 1.15 cm, which is far less than 1.8 cm of fuzzy PID control, which is about 36%; the adjustment change of horizontal traction force is 1293.35 N, which is less than 2217 N of fuzzy PID control, which is about 42%. When the tractor realizes the optimal value control of slip rate, the adjustment amount is small, which makes the tractor keep in a more stable working state.

- **Control target value with pulse change**

The test conditions are set as above, and the results are shown in figure 10.

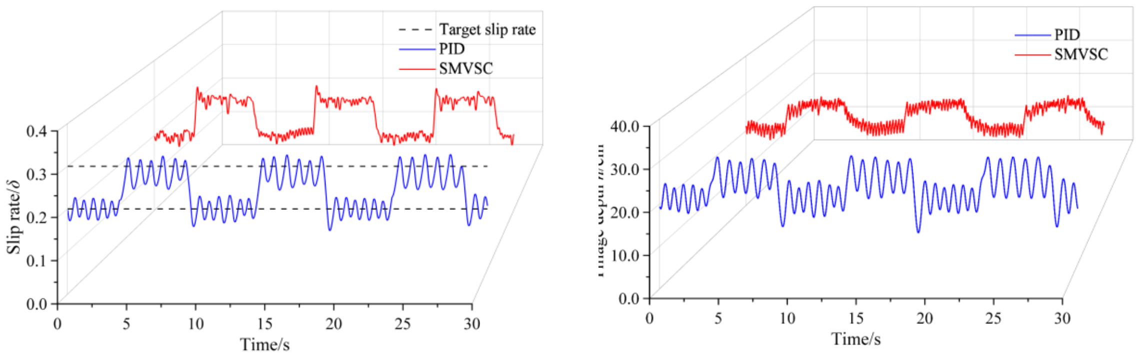

(a) The result of slip rate *(b) The result of tillage depth*

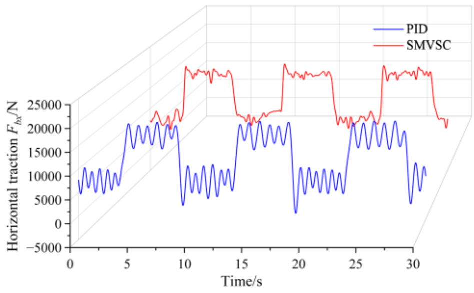

(c) The result of horizontal traction

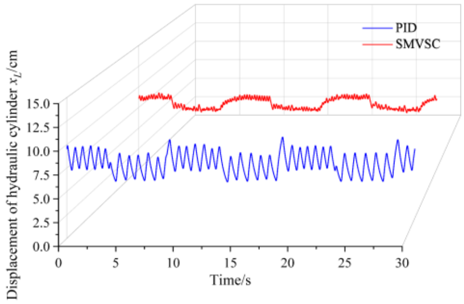

(d) The result of hydraulic cylinder displacement

Fig. 10 - HILS results of control target value with pulse change

When the slip rate control target changes between 0.2 and 0.3, both algorithms can effectively track the dynamically changing slip rate target value, but the tracking response time of SMVSC method is reduced by about 0.8s less than that of fuzzy PID control, the average control overshoot is reduced by about 0.03, and the control deviation and fluctuation range are also significantly reduced. At the same time, the results by the SMVSC method show that, the displacement of the tractor hydraulic lift cylinder and the adjustment depth of the ploughing depth are significantly smaller than those obtained by the fuzzy PID control, and the fluctuation range of the horizontal traction force is also significantly reduced.

Compared with the integrated traction-slip ratio control method previously proposed by our team *(Zhang et al., 2016)*, the slip ratio control strategy developed in this study achieved superior target slip ratio tracking performance while maintaining minimal fluctuations in tillage depth and traction force. The proposed SMVSV method demonstrated significant improvements over existing slip ratio control approaches *(Bai et al., 2012; Soylu et al., 2021)*, reducing the system response time to within 1 second, decreasing the mean absolute deviation of slip ratio to 0.014 under soil specific resistance with pulse change, and significantly minimizing slip ratio overshoots along with fluctuations in tillage depth and traction force during target slip ratio adjustments with pulse change.

It can be seen that the method based on SMVSC has shorter response time, smaller control overshoot, and better dynamic tracking performance in the slip control process. As a robust control method, the control process of SMVSC method is independent of the state of the system and external disturbances, it has the advantages of parameter disturbance insensitivity and simple implementation. In view of the strong nonlinear and complex coupling characteristics of heavy tractor ploughing unit, SMVSC method has certain control advantages and better control effect than fuzzy PID control. While controlling the slip rate to the target value, the adjustment amount is smaller, which can maintain a more stable tractor field working condition.

CONCLUSIONS

(1) For the ploughing operation conditions, considering the nonlinear characteristics of the complex coupling system of the "tractor-tools-soil", a time-varying nonlinear dynamic model of the tractor's electro-hydraulic hitch system was developed, and the nonlinear motion characteristics of the system were clarified.

(2) Based on the theory of Sliding Mode Variable Structure Control (SMVSC), considering the strong nonlinearity, time-variability, and uncertainty characteristics of the dynamic system, the piston pressure in the hydraulic cylinder was selected as the control variable. A slip control algorithm for the tractor's drive wheels was designed, with a fuzzy PID algorithm used as a comparative benchmark. Simulations and analyses were conducted in MATLAB/Simulink.

(3) A hardware-in-the-loop simulation (HILS) test platform was developed to over-come the limitations of field experiment and to evaluate the real-time execution capabilities of the control algorithm. The results indicated that the SMVSC algorithm effectively achieved optimal slip rate control and a more stable operational state within the electro-hydraulic hitch system, characterized by reduced adjustment amplitudes. This advancement is significant for minimizing energy consumption and enhancing the quality of ploughing activities during operations.

ACKNOWLEDGEMENT

This research was supported by the National Natural Science Foundation of China (No.32201677), the Shaanxi Key Research Development Project (2023-ZDLNY-62, 2024NC-YBXM-202, 2024NC-YBXM-244).

REFERENCES

[1] Bai X., Lu Z., Chang J., Li H., Zhou W. (2012) Fuzzy Control Algorithm Simulation of Automatic Control of Tilling Depth for Tractor Based on Slip Rate. *Transactions of the Chinese Society for Agricultural Machinery*. Vol. 43, pp. 6–10. China.

[2] Ding C., Ding S., Wei X., Mei K. (2022) Composite SOSM Controller for Path Tracking Control of Agricultural Tractors Subject to Wheel Slip. *ISA Transactions*, Vol. 130, pp. 389–398. China.

[3] Giller K.E., Andersson J.A., Corbeels M., Kirkegaard J., Mortensen D., Erenstein O., Vanlauwe B. (2015). Beyond Conservation Agriculture. *Frontiers in Plant Science*, Vol. 6. Netherlands.

[4] Holthusen D., Brandt A.A., Reichert J.M., Horn R., Fleige H., Zink A. (2018). Soil Functions and in Situ Stress Distribution in Subtropical Soils as Affected by Land Use, Vehicle Type, Tire Inflation Pressure and Plant Residue Removal. *Soil & Tillage Research*, Vol. 184, pp. 78–92. Brazil.

[5] He Z., Song Z., Wang L., Zhou X., Gao J., Wang K., Yang M., Li Z. (2023). Fasting the Stabilization Response for Prevention of Tractor Rollover Using Active Steering: Controller Parameter Optimization and Real-Vehicle Dynamic Tests. *Computers and Electronics in Agriculture,* Vol. 204, 107525. China.

[6] Janulevičius A., Šarauskis E., Čiplienė A., Juostas A. (2019). Estimation of Farm Tractor Performance as a Function of Time Efficiency during Ploughing in Fields of Different Sizes. *Biosystems Engineering*, Vol. 179, pp. 80–93. Republic of Lithuania.

[7] Ji X., Ding S., Wei X., Cui B. (2023) Path tracking of unmanned agricultural tractors based on a novel adaptive second-order sliding mode control. *Journal of the Franklin Institute*, Vol. 360(8), pp. 5811-5831.

[8] Li S., Wang J., Li K. (2007). Design and Development of the Monitoring System for Hardware-in-the-Loop Simulation Test Bench. *Systems Engineering Procedia*, Vol. 19(16), pp. 3684–3687. China.

[9] Pranav P.K., Pandey K.P., Tewari V.K. (2010). Digital Wheel Slipmeter for Agricultural 2WD Tractors. *Computers and Electronics in Agriculture*, Vol. 73, pp. 188–193. India.

[10] Paksoy M. (2020). Nonlinear Adaptive Semiactive Control of a Half-Vehicle Model via Hardware in the Loop Simulation. *Turkish Journal of Electrical Engineering and Computer Sciences*, Vol. 28, pp. 1612–1630. Turkey.

[11] Raikwar S., Jijyabhau Wani L., Arun Kumar S., Sreenivasulu Rao M. (2019). Hardware-in-the-Loop Test Automation of Embedded Systems for Agricultural Tractors. *Measurement*, Vol. 133, pp. 271–280.

[12] Rahmati M., Eskandari I., Kouselou M., Feiziasl V., Mahdavinia G.R., Aliasgharzad N., McKenzie B.M. (2020). Changes in Soil Organic Carbon Fractions and Residence Time Five Years after Implementing Conventional and Conservation Tillage Practices. *Soil & Tillage Research*, 200, 104632.

[13] Soylu S. , Arman K. . (2021). Fuzzy logic based automatic slip control system for agricultural tractors. *Journal of Terramechanics*, Vol. 95(7), pp. 25-32. Turkey.

[14] Watanabe M., Sakai K. (2019). Impact Dynamics Model for a Nonlinear Bouncing Tractor during Inclined Passage. *Biosystems Engineering*, Vol. 182, pp. 84–94. Japan.

[15] Wu Z., Xie B., Li Z., Mitsuoka M., Inoue E., Okayasu T., Hirai Y. (2019). dSPACE Based Hardware in the Loop Testing Platform for Powertrain Management Unit of Electric Tractor. *Journal of the Faculty of Agriculture, Kyushu University*, Vol 64, pp. 309–317. China.

[16] Wang Y., Chen S., Zhang D., Yang L., Cui T., Jing H., Li Y. (2020). Effects of Subsoiling Depth, Period *Journal of Integrative Agriculture*, Vol. 19, pp. 1596–1608. China.

[17] Xu G., Chen M., He X., Pang H., Miao H., Cui P., Wang W., Diao P. (2021). Path Following Control of Tractor with an Electro-Hydraulic Coupling Steering System: Layered Multi-Loop Robust Control Architecture. *Biosystems Engineering*, Vol 209, pp. 282–299. China.

[18] Zhang S., Du Y., Zhu Z., Mao E., Liu J., Shi J. (2016). Integrated control method of traction & slip ratio for rear-driving high-power tractors. *Trans. Chinese Society of Agricultural Engineering*, Vol. 32(12), pp. 47-53. China.

[19] Zhang S., Wu Z., Chen J., Li Z., Zhu Z., Song Z., Mao E. (2020). Control method of driving wheel slip rate of high-power tractor for ploughing operation. *Transactions of the Chinese Society of Agricultural Engineering*, Vol 36(15), pp. 47-55. China.

[20] Zhang T., Jiao X., Lin Z. (2022) Finite Time Trajectory Tracking Control of Autonomous Agricultural Tractor Integrated Nonsingular Fast Terminal Sliding Mode and Disturbance Observer. *Biosystems Engineering*, Vol. 219, pp. 153–164. China.

[21] Zhang S., Wen C., Ren W., Luo Z., Xie B., Zhu Z., Chen Z. (2023). A Joint Control Method Considering Travel Speed and Slip for Reducing Energy Consumption of Rear Wheel Independent Drive Electric Tractor in Ploughing. *Energy*, Vol. 263, 126008. China.